

DOI: 10.1002/ ((please add manuscript number))

**Article type:** Full paper

**Towards high thermoelectric performance of thiophene and ethylenedioxythiophene (EDOT) molecular wires.**

Marjan Famili <sup>\*a</sup>, Iain M. Grace <sup>a</sup>, Qusiy Al-Galiby <sup>b</sup>, Hatef Sadeghi <sup>a</sup>, Colin J. Lambert <sup>a\*</sup>

<sup>a</sup>Physics Department, Lancaster University, Lancaster, United Kingdom, LA1 4YB

<sup>b</sup>Department of Physics, College of Education, University of Al-Qadisiyah, Diwaniyah, 58002, Iraq

\* [m.famili@lancaster.ac.uk](mailto:m.famili@lancaster.ac.uk), [c.lambert@lancaster.ac.uk](mailto:c.lambert@lancaster.ac.uk)

**Keywords:** Thermoelectricity, figure of merit, molecular wire, thiophene, EDOT, ZT

**Abstract:**

The design of thermoelectric materials for the efficient conversion of waste heat into electricity requires simultaneous tuning of their electrical and thermal conductance. Here we perform a comparative theoretical study of electron and phonon transport in thiophene and ethylenedioxythiophene (EDOT) based molecular wires. We show that modifying thiophene by substituting ethylenedioxy, enhances the thermoelectric figure of merit  $ZT$  for molecules of the same length. Furthermore, we demonstrate that the electrical conductance of EDOT-based wires decays more slowly with length than that of thiophene-based wires and that their thermal conductance is lower. The room-temperature  $ZT$  of undoped EDOT was found to be rather low. However, doping of EDOT by the electron acceptor toluenesulfonate (TOS) increases the Seebeck coefficient and electrical conductance, while decreasing the thermal conductance, leading to a thermoelectric figure of merit as high as  $ZT=2.4$ .

## 1. Introduction

The attraction of single-molecule electronics has arisen from their potential for sub-10nm electronic switches and rectifiers and from their provision of sensitive platforms for single-molecule sensing.<sup>[1-17]</sup> In recent years, the potential of self-assembled monolayers for removing heat from nanoelectronic devices and thermoelectrically converting waste heat into electricity has also been recognized.<sup>[18-29]</sup> The key property characterising the efficiency at which thermal energy is converted into electrical energy is the dimensionless thermoelectric figure of merit  $ZT = GS^2T/\kappa$ , where  $G$  is the electrical conductance,  $S$  is the Seebeck coefficient,  $T$  is temperature and  $\kappa$  is the thermal conductance. Therefore optimisation of  $ZT$  requires design of materials, which maximise the numerator (ie the power factor  $GS^2$ ) and simultaneously minimise the denominator (ie the thermal conductance). The current world record for inorganic materials is  $ZT \approx 2.2$  at temperatures over 900 K.<sup>[28,29]</sup> However, this low level of efficiency means that the widespread use of thermoelectricity for energy harvesting is not economic. Organic thermoelectric materials may be an attractive alternative, but at present the best organic thermoelectric materials have a  $ZT = 0.42$  at room temperature,<sup>[30,31]</sup> which is still too low. To overcome this barrier, several groups are now attempting to identify design strategies for optimising the thermoelectric properties of single molecules, with a view to subsequent translation of their enhanced functionality to self-assembled molecular layers.

Strategies for increasing the power factor  $GS^2$  of single-molecule junctions focus on optimising electron transport properties by tuning the energetic position of the frontier orbitals of the molecule relative to the Fermi energy  $E_F$  of the electrodes. If  $T_{el}(E)$  is the transmission coefficient of electrons of energy  $E$  passing from one electrode to the other through a molecule, then the Seebeck coefficient  $S$  is approximately proportional to the slope of the  $-\ln T_{el}(E)$ , evaluated at  $E_F$ , whereas the electrical conductance is proportional to  $T_{el}(E_F)$ .

Therefore, it is favourable to use molecular design to control the position of the resonances in  $T_{el}(E)$ , which occur when the electron energy  $E$  coincides with a molecular energy level.<sup>[48-50]</sup>

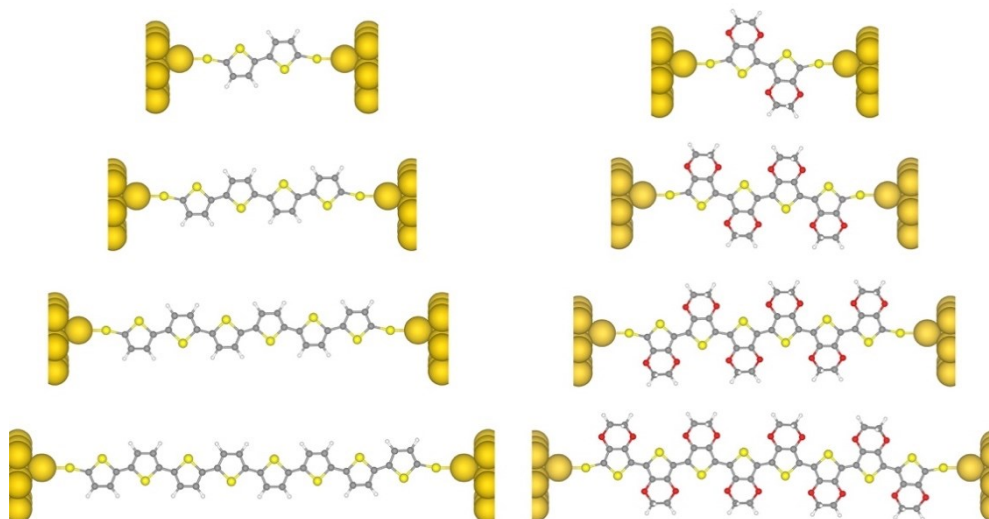


**Figure 1.** Optimised geometry of the thiophene series (left) and EDOT series (right) for  $n = 1$  to 4 units contacted between gold electrodes.

The thermoelectric properties of bulk oligothiophene derivatives have received attention,<sup>[30-42]</sup> due to their conjugated nature, which provides  $\pi$  orbital overlap along the backbone of the molecule and favours electron transport. Moreover, chemical modification of the oligothiophenes can be used as a tool to improve their conductance.<sup>[8,35-42]</sup> Ethylenedioxythiophene (EDOT) is a derivative of thiophene obtained by ethylenedioxy substitution, which in its polymeric form is reported to reduce the charge carrier effective mass and the HOMO-LUMO gap.<sup>[35,41,42]</sup> The EDOT based organic polymer, in its doped form (PEDOT:PSS) has the highest recorded  $ZT = 0.42$  for a bulk organic semiconductor.<sup>[30,31,39]</sup> Here we calculate and compare the  $ZT$  of a family of oligothiophene and EDOT-based single-molecule junctions as a function of their length. Our calculations reveal that in all cases, the  $ZT$  of EDOT exceeds that of the corresponding oligothiophenes. Furthermore, we demonstrate that doping the EDOT monomer with the electron acceptor

toluenesulfonate (TOS), which is the building block of PSS,<sup>[31]</sup> results in significant improvement of  $ZT$ .

## 2. Theoretical Method

To investigate the thermal efficiency of these two series of molecules, we computed both electron and phonon transport properties of the molecular junctions shown in figure 1. To compute their electronic properties the isolated molecules were first relaxed to an optimum configuration using the density functional theory (DFT) code SIESTA<sup>[43]</sup>, so that all the forces on the atoms were less than  $0.01 \text{ eV/\AA}$ . A double-zeta plus polarization basis set, norm conserving pseudo potentials and a real space grid cut off of 185 Rydbergs were employed and the GGA<sup>[44]</sup> was used as the exchange correlation. An extended molecule was then constructed by introducing gold electrodes as shown in figure 1, and further relaxing the junction. The optimised sulfur-gold distance was found to be  $2.5 \text{ \AA}$  in all calculations. From this converged DFT calculation, the underlying mean-field Hamiltonian  $H$  was combined with our quantum transport code, GOLLUM to obtain the transmission coefficient  $T_{el}(E)$  for electrons of energy  $E$  passing from one electrode to the other. Using the approach presented in reference [45], the electrical conductance  $G_{el}(T) = G_0 L_0$ , the electronic contribution of the thermal conductance  $\kappa_e(T) = (L_0 L_2 - L_{12})/h T L_0$  and the Seebeck coefficient  $S(T) = -L_1/e T L_0$  of the junction were calculated from the moments

$$L_n(T) = \int_{-\infty}^{+\infty} dE (E - E_F)^n T_{el}(E) \left( -\frac{\partial f_{FD}(E, T)}{\partial E} \right) \quad (1)$$

In the above expression,  $f_{FD}(E, T)$  is the Fermi–Dirac probability distribution function  $f_{FD}(E, T) = (e^{(E-E_F)/k_B T} + 1)^{-1}$ ,  $T$  is the temperature,  $E_F$  is the Fermi energy,  $G_0 = 2e^2/h$  is the conductance quantum,  $e$  is electron charge, and  $h$  is the Planck’s constant.

To calculate the thermal conductance due to phonons, the interatomic force matrix  $K$  was obtained from the second derivatives at equilibrium of the total energy with respect to the displacements; ie

$$K_{i\alpha,j\beta} = \frac{\partial^2 U}{\partial r_{i\alpha} \partial r_{j\beta}} \quad (2)$$

where  $i$  and  $j$  label atomic sites,  $\alpha$  and  $\beta$  are Cartesian coordinates and  $U$  is the total energy.

Within the harmonic approximation, the above equation can be written

$$K_{i\alpha,j\beta} = \frac{F_{j\beta}(d_{i\alpha}) - F_{j\beta}(d_{i\alpha})}{2d_{i\alpha}} \quad (3)$$

where  $d_{i\alpha}$  is the displacement of atom  $i$  (0.01 Å in the current study) in the direction of  $\alpha(x, y, z)$  and  $F_{j\beta}$  is the resultant force on atom  $j$  due to displacement of atom  $i$ . The corresponding dynamical matrix is,

$$D_{i\alpha,j\beta} = \frac{K_{i\alpha,j\beta}}{\sqrt{M_i M_j}} \quad (4)$$

where  $M_i$  is the mass of atom  $i$ . Finally, to ensure the conservation of momentum, we correct the dynamical matrix such that  $K_{ii} = -\sum_{i \neq j} K_{ij}$ . The transmission probability for phonons through the junction is then given by <sup>[45]</sup>

$$T_{ph}(\omega) = \text{Trace}[(G^r(\omega)\Gamma_R(\omega)G^{r\dagger}(\omega)\Gamma_R(\omega))] \quad (5)$$

In the above equation  $\Gamma_{R,L}$  describe the level broadening of phonon modes due to the left and right contacts of leads and molecule, and  $G^{r\dagger}(\omega)$  and  $G^r(\omega)$  are advanced and retarded phonon Green's functions. From this equation, the contribution to the thermal conductance  $\kappa_{ph}(T)$  due to phonons is given by

$$\kappa_{ph}(T) = \frac{1}{2\pi} \int_0^\infty \hbar \omega T_{ph}(\omega) \frac{\partial f_{BE}(\omega, T)}{\partial T} d\omega \quad (6)$$

where  $f_{BE}(\omega, T) = (e^{\hbar\omega/k_B T} - 1)^{-1}$  is the Bose–Einstein distribution function.

### 3. Results

The calculated room-temperature electrical conductances for the two series of thiophene and EDOT-based wires are shown in Figures 2a and 2b respectively. The DFT-predicted Fermi energy ( $E_F - E_F^{DFT} = 0$  eV) sits close to the HOMO resonance in both cases and would lead to high conductance values (T1 has a value of  $0.47 G_0$  and E1  $0.48 G_0$ ). Experimental measurements on a thiophene series show a measured conductance value of  $G = 3 * 10^{-3} G_0$  and a Seebeck coefficient of  $S = 8 \mu V/K$  for molecule T1.<sup>[33]</sup> The discrepancy arises from the incorrect energy level alignment of the molecules with the Fermi energy of gold leads. This is a known problem in DFT-based quantum transport calculations and leads to overestimation of the conductance. Various methods have been employed to correct this including the DFT+ $\Sigma$ <sup>[46]</sup> and scissor corrections.<sup>[47]</sup> In the case of thiol based anchor groups, where the molecule desorbs a hydrogen atom on the gold, the application of these corrections is somewhat subjective, since the molecule without hydrogens does not exist in the gas phase. Therefore, in what follows, we use the measured conductance and Seebeck coefficient of T1 molecule to locate the relative position of the HOMO. Shifting the DFT predicted Fermi energy to  $E_F - E_F^{DFT} = 0.35$  eV yields  $G = 8 * 10^{-3} G_0$  and  $S = 20.3 \mu V/k$ , which is in reasonable agreement with the experimental measurements. Therefore, in what follows, we adopt this value of Fermi energy.

Figure 2c shows the conductance  $\ln(G/G_0)$  vs  $L$  for the four different lengths of EDOT (red) and thiophene (black), and as expected for coherent tunnelling, we find a clear exponential decrease of conductance with oligomer length in both cases ( $G \sim e^{-\beta L}$ ). Figure 2d shows the beta-factor obtained from the slopes of such plots at different Fermi energies ( $E_F$ ), and

demonstrates that the beta-factor of the EDOT series (E1-E4) is lower than that of thiophene ( $1 \text{ nm}^{-1}$  to  $1.75 \text{ nm}^{-1}$  respectively) over a range of Fermi energies in the vicinity of our chosen Fermi energy  $E_F - E_F^{DFT} = 0.35 \text{ eV}$ . Figures 2a and 2b show that the off-resonant conductance in the HOMO-LUMO gap is lower for the thiophene, due to the fact that the EDOT has a smaller HOMO-LUMO gap. This mirrors the comparable behaviour in polymers [35] and suggests that the observed reduction in the HOMO-LUMO gap is purely due to the chemical modification of the molecule. As noted in [35], the donor-type ethylenedioxy substitution causes anti-bonding interactions between the O and C on the molecule backbone, which destabilizes both HOMO and LUMO and leads to reduction of the gap.

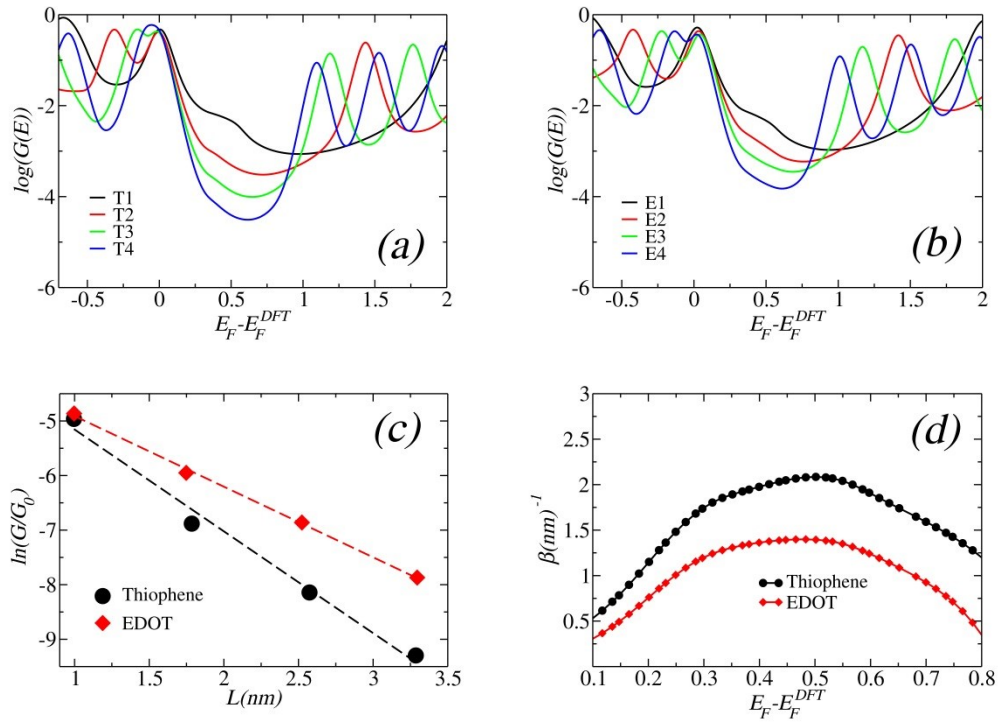


**Figure 2.** Room temperature conductance for the (a) thiophene (a) and (b) EDOT molecular wires shown in figure 1. (c) Conductance vs length at  $E_F - E_F^{DFT} = 0.35 \text{ eV}$ . (d) Beta factor vs Fermi energy. The predicted value for the decay constant of oligothiophene is somewhat lower than the experimental value of  $\beta = 2.9 \text{ nm}^{-1}$ , [9,33] because DFT underestimates the HOMO-LUMO gap.

To optimise the numerator of  $ZT$ , we next investigate the Seebeck coefficient  $S$ . The value of  $S$  is proportional to the slope of the transmission at the Fermi Energy. This means that  $S$  is high when  $E_F$  is greater than the energy of HOMO resonance and smaller than the energy of the middle of the HOMO-LUMO gap. Figure 3 shows a comparison between the Seebeck coefficient of the thiophene and EDOT series in the vicinity of  $E_F - E_F^{DFT} = 0.35 \text{ eV}$ . For the same length of oligomer, the Seebeck coefficients of the EDOT series are lower than those of the thiophene series, because the higher HOMO-LUMO gap of the former leads to a lower mid-gap transmission coefficient and therefore to a higher slope. Figure 3 also demonstrates that in both molecular series,  $S$  increases with molecular length in agreement with previous work.<sup>[33,34]</sup> As shown in figure 3, this trend is not dependent on the value of the Fermi energy.

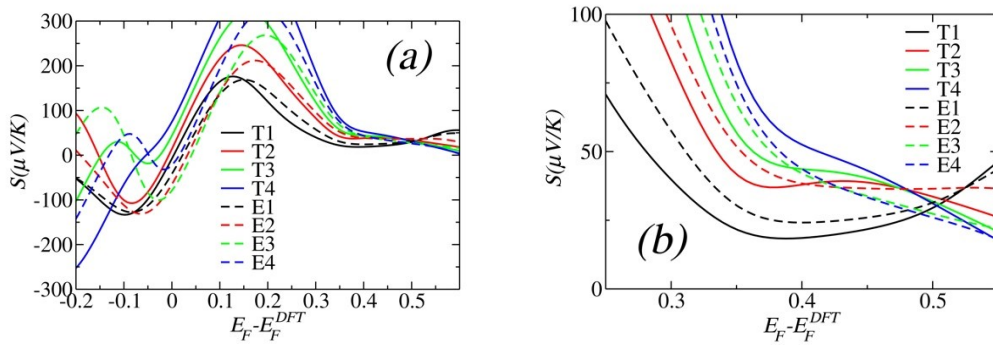


**Figure 3.** Seebeck coefficient  $S$  against Fermi energy for thiophenes and EDOTs over a range of  $-0.2 < E_F - E_F^{DFT} < 0.6$  (b) Seebeck coefficient over a range of Fermi energy in the vicinity of chosen Fermi energy  $E_F - E_F^{DFT} = 0.35 \text{ eV}$

The thermal conductance  $\kappa = \kappa_e + \kappa_{ph}$  in the denominator of  $ZT$  is composed of two terms; the thermal conductance due to electrons ( $\kappa_e$ ) and the thermal conductance due to phonons ( $\kappa_{ph}$ ). Comparison between figure 4a and figure 4b reveals that the phonon contribution is greater than the electronic contribution. However the ratio  $\kappa_{ph}/\kappa_e$  is lower for the EDOT series than for the thiophene series, which makes the former more attractive for



thermoelectricity. This is due to the higher value of  $\kappa_{ph}$  for thiophenes, which arises from rotational vibrational modes of the thiophene rings. These become more restricted after ethylenedioxy substitution and the phonon conductance of the EDOT series is lower than that of the thiophene series.<sup>[51]</sup> The change in phonon thermal conductance with length arises from a balance between two competing factors. The first is a narrowing of the phonon transmission resonances with increasing length, which reduces the thermal conductance. The second is an increase with length of the number of phonon modes below the Debye frequency of the electrodes, which tends to increase the thermal conductance.<sup>[52]</sup> As a result of this competition, for the EDOT series, although the longer molecules E3 and E4 have a lower thermal conductance than the shorter molecules E1 and E2, there is very little difference between E1 and E2, whilst E4 has very slightly higher thermal conductivity than E3. Similarly for the thiophene series, the phonon conductance of T2 is lower than that of T1, as expected. However, the thermal conductance then increases for T3 and T4, because due to mode softening, the number of modes entering the Debye window dominates. Similar non-conventional behaviour has been observed in recent measurements of alkane chains.<sup>[53]</sup> Phonon transmission curves and open channels are presented in the SI.

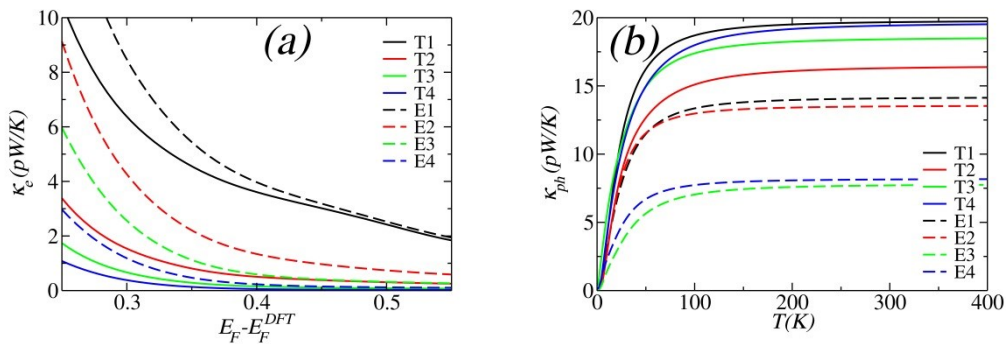


**Figure 4.** (a) The electronic thermal conductance at 300 K over a range of  $E_F - E_F^{DFT}$  (b) the phonon thermal conductance of both the EDOT and thiophene series.

Figure 5 shows the resulting thermoelectric figure of merit  $ZT$ . At the benchmarked Fermi energy of  $E_F - E_F^{DFT} = 0.35$  eV the value of  $ZT$  is much less than 1. However, at lower values of the Fermi energy,  $ZT$  of molecule E4 is as high as 3, because the system is closer to the HOMO resonance.

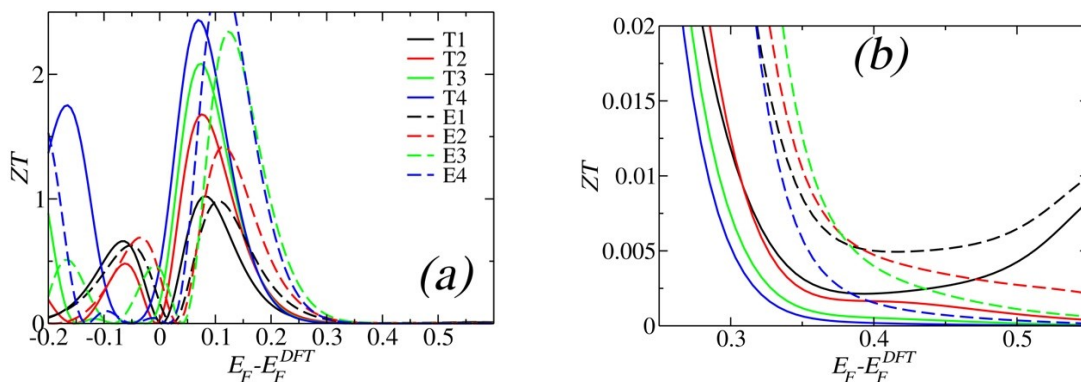


**Figure 5.** (a)  $ZT$  in a range of Fermi energy from -0.2 to 0.6 (b)  $ZT$  over a range of Fermi energy in the vicinity of chosen Fermi energy  $E_F - E_F^{DFT} = 0.35$  eV

This suggests that  $ZT$  could be enhanced by doping with an electron acceptor, which would cause the molecular energy levels to increase in energy relative to the Fermi energy. To investigate the tuneability of  $ZT$  via doping, we have doped the EDOT monomer (E3) with toluenesulfonate(TOS) which is an electron acceptor agent. The charge transfer process in an EDOT:TOS complex is discussed at length in the

literature.[31]

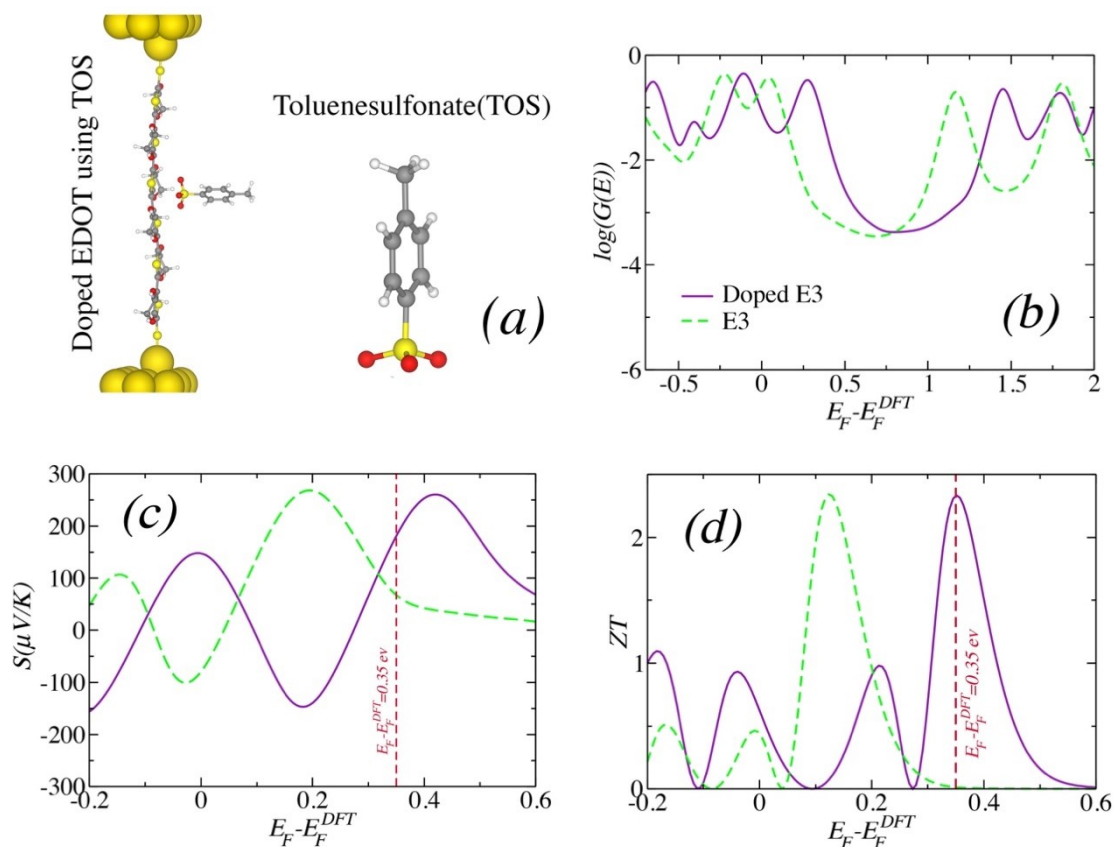


**Figure 6.** (a) Toluenesulfonate (TOS) and EDOT:TOS in the junction and the comparison between the logarithm of conductance (b), Seebeck coefficient (c) and the  $ZT$  (d) of E3 in a doped and undoped state.

The gold electrodes are the same in both calculations (with and without the dopant). Therefore, the Fermi energy is kept constant for both calculations and is  $E_F - E_F^{DFT} = 0.35 \text{ eV}$ . As expected, doping shifts the HOMO and LUMO hence bringing a higher slope towards the Fermi energy which leads to a significantly larger Seebeck coefficient and electrical conductance. This results in a  $ZT$  value of 2.4.

#### 4. Conclusion

We have studied the length dependence of the thermoelectric properties of thiophene and EDOT molecular wires. By converting the basic thiophene unit to EDOT, where a thiophene oligomer is

modified by adding ethylenedioxy, we have demonstrated that the electronic conductance decay factor is smaller for EDOT and its thermal conductance is lower. Consequently, the thermoelectric performance of EDOT exceeds that of the corresponding oligothiophenes for all lengths studied. The room-temperature  $ZT$  of undoped EDOT was found to be rather low. However, doping of EDOT by the electron acceptor toluenesulfonate(TOS), which moves the HOMO closer to the Fermi energy leads to room-temperature  $ZT$  values as high as 2.4. In addition to chemical modifications and length dependence considered above, we expect different binding groups to play a role and therefore each new series of molecules must be studied in detail to ascertain their suitability for thermoelectricity. As an example, figure S4 of the SI shows that replacing the thiol anchors with thiol-methyl (SME) tilts the geometry of the E1 molecule in the junction, creating larger  $\Gamma_{R,L}$  with the gold. This leads to higher phonon conductance, which is not desirable. For this reason, we have focussed on molecules with thiol anchor groups.

## Supporting Information

Supporting Information is available from the Wiley Online Library or from the author.

## Acknowledgements

This work was also supported by UK EPSRC grant nos. EP/N017188/1, EP/M014452/1 and EP/N03337X/1, and the EC FP7 ITN Molecular-Scale Electronics “MOLESCO” project no. 606728.

Received: ((will be filled in by the editorial staff))

Revised: ((will be filled in by the editorial staff))

Published online: ((will be filled in by the editorial staff))

## References

- [1] C. J. Lambert, Chem. Soc. Rev. **2015**, 44,4.
- [2] P. Gehring, J. K. Sowa, J. Cremers, Q. Wu, H. Sadeghi, Y. Sheng, J. H. Warner, C. J. Lambert, G. A. D. Briggs and J. A. Mol, ACS Nano, **2017**, 11, 6.
- [3] M. Bürkle, L. Zotti, J. Viljas, D. Vonlanthen, A. Mishchenko, T. Wandlowski, M. Mayor, G. Schön, and F. Pauly, Phys. Rev. B, **2012**, 86, 11.
- [4] S. K. Yee, J. A. Malen, A. Majumdar, and R. A. Segalman, Nano Lett. **2011**, 11, 10.
- [5] S. K. Lee, T. Ohto, R. Yamada, and H. Tada, Nano Lett. **2014**, 14, 9.
- [6] A. Tan, J. Balachandran, S. Sadat, V. Gavini, B. D. Dunietz, S.-Y. Jang, and P. Reddy, J. Am. Chem. Soc. **2011**, 133, 23.
- [7] J. Balachandran and P. Reddy, J. Phys. Chem. Lett. **2012**, 3, 15.
- [8] J. R. Widawsky, W. Chen, H. Vázquez, T. Kim, R. Breslow, M. S. Hybertsen, and L. Venkataraman, Nano Lett. **2013**, 13, 6.
- [9] W. B. Chang, C. Mai, M. Kotiuga, J. B. Neaton, G. C. Bazan, and R. A. Segalman, Chem. Mater. **2014**, 26, 24.
- [10] C. Evangeli, K. Gillemot, E. Leary, M. T. González, G. Rubio-Bollinger, C. J. Lambert, and N. Agraït, Nano Lett. **2013**, 13, 5.
- [11] Y. Kim, W. Jeong, K. Kim, W. Lee, and P. Reddy, Nat. Nanotechnol. **2014**, 9, 11.
- [12] V. M. García-Suárez, C. J. Lambert, D. Z. Manrique and T. Wandlowski, Nanotech. **2014**, 25.
- [13] L. Rincón-García, A. K. Ismael, C. Evangeli, I. Grace, G. Rubio-Bollinger, K. Porfyrakis, N. Agraït, and C. J. Lambert, Nature Mater. **2016**, 15, 289.
- [14] Q. Al-Galiby, H. Sadeghi, and L. Algharagholy, Nanoscale. **2016**.
- [15] J. A. Malen, S. K. Yee, A. Majumdar, and R. a. Segalman, Chem. Phys. Lett. **2010**, 491, 4–6.

- [16] J. R. Widawsky, P. Darancet, J. B. Neaton, and L. Venkataraman, *Nano Lett.* **2012**, 12, 1.
- [17] L. D. Zhao, V. P. Dravid, and M. G. Kanatzidis, *Energy Environ. Sci.* **2014**, 7, 1.
- [18] Q. Zhang, Y. Sun, W. Xu, and D. Zhu, *Adv. Mater.* **2014**, 26, 40.
- [19] H. Shi, C. Liu, J. Xu, and H. Song, *Int. J. Electrochem. Sci.* **2014**, 9.
- [20] M. Sumino, K. Harada, M. Ikeda, S. Tanaka, K. Miyazaki, and C. Adachi, *Appl. Phys. Lett.* **2011**, 99, 9.
- [21] H. Akkerman, P. Blom, D. De Leeuw, and B. De Boer, *Nature*, **2006**, 441, 69.
- [22] T. Li, J. Hauptmann, and Z. Wei, *Adv. Mater.* **2012**, 24, 10.
- [23] G. Wang, Y. Kim, M. Choe, T.W. Kim, and T. Lee, *Adv. Mater.* **2011**, 23, 6.
- [24] A. Neuhausen and A. Hosseini, *ACS Nano*. **2012**, 11, 9920.
- [25] S. Majumdar, J. A. Sierra-Suarez, S. N. Schiffres, W.-L. Ong, C. F. Higgs, A. J. H. McGaughey, and J. A. Malen, *Nano Lett.* **2015**, 15, 5.
- [26] R. Y. Wang, R. A. Segalman, and A. Majumdar, *Appl. Phys. Lett.* **2006**, 89, 17.
- [27] G. Kiršanskas, Q. Li, K. Flensberg, G. C. Solomon, and M. Leijnse, *Appl. Phys. Lett.* **2014**, 105, 23, 233.
- [28] G. J. Snyder and E. S. Toberer, *Nat. Mater.* **2008**, 7, 105.
- [29] R. Venkatasubramanian, E. Siivola, T. Colpitts and B. O'Quinn, *Nature*, **2001**, 413, 597.
- [30] G. Kim, L. Shao, K. Zhang, and K. Pipe, *Nat. Mater.* **2013**, 12, 8.
- [31] O. Bubnova, et al., , *Nat. Mater.* **2011**, 10, 429.
- [32] E. J. Dell, B. Capozzi, J. Xia, L. Venkataraman, and L. M. Campos, *Nat Chem.* **2015**, 7, 209.
- [33] B. Capozzi, E. J. Dell, T. C. Berkelbach, D. R. Reichman, L. Venkataraman, L. M. Campos, *J. Am. Chem. Soc.* **2014**, 136, 29.
- [34] R. Yamada, H. Kumazawa, T. Noutoshi, S. Tanaka, and H. Tada, *Nano Lett.* **2008**, vol. 8, no. 4, pp. 1237.

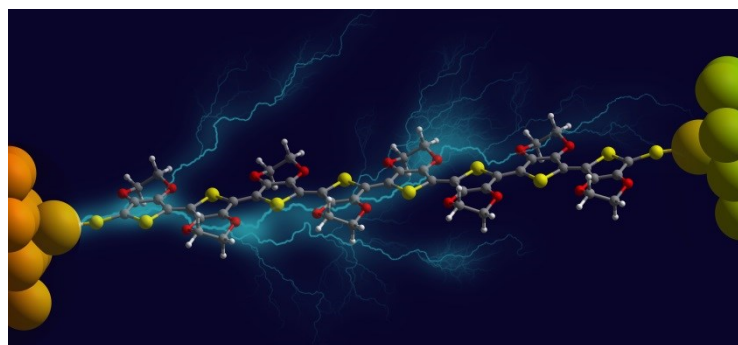
- [35] E. Kim and J. Bredas, *J. Am. Chem. Soc.* **2008**, 130, 50.
- [36] S. Potash and S. Rozen, *Chem. A Euro. J.* **2013**, 19, 17.
- [37] P. Pingel, Richard Schwarzl, and Dieter Neher, *Appl. Phys. Lett.* **2012**, 100.
- [38] M. Schubert, E. Preis, J. C. Blakesley, P. Pingel, U. Scherf, and D. Neher, *Phys. Rev. B.* **2013**, 87.
- [39] G. Lu, J. Blakesley, S. Himmelberger, P. Pingel, J. Frisch, I. Lieberwirth, I. Salzmann, M. Oehzelt, R. di Pietro, A. Salleo, N. Koch, and D. Neher, *Nat. Commun.* **2013**, 4, 1588.
- [40] J. Roncali, P. Blanchard and P. Frere, *J. Mater. Chem.* **2005**, 15.
- [41] R. Gangopadhyay, B. Das, and M. Molla, *Rsc. Adv.* **2014**, 4, 83.
- [42] O. Bubnova, Z. Khan, H. Wang, S. Braun, D. R. Evans, M. Fabretto, H. Pejman, D. Dagnelund, J. Arlin, Y. H. Geerts, S. Desbief, D. W. Breiby, J. W. Andreasen, R. Lazzaroni, W. M. Chen, I. Zozoulenko, M. Fahlman, P. J. Murphy, M. Berggren, and X. Crispin, *Nat. Mater.* **2014**, 13, 2.
- [43] J. M. Soler, E. Artacho, J. D. Gale, A. García, J. Junquera, P. Ordejón, and D. Sánchez-Portal, *J. Phys. Condens. Matt.* **2002**, 14, 2745.
- [44] J. P. Perdew, K. Burke, and M. Ernzerhof, *Phys. Rev. Lett.* **1996**, 77, 3865.
- [45] J. Ferrer, C. Lambert, V. Garcia-Suarez, D. Z. Manrique, D. Visontai, L. Oroszlany, R. Ferradas, I. Grace, S. Bailey, K. Gillemot, H. Sadeghi, L. Algharagholy, *New J. Phys.* **2014**, 16, 093.
- [46] J. B. Neaton, M. S. Hybertsen, and S. G. Louie, *Phys. Rev. Lett.* **2006**, 97.
- [47] V. M. Garcia-Suarez and C.J. Lambert, *New J. Phys.* **2011**, 13.

- [48] X. Liu, S. Sangtarash, D. Reber, D. Zhang, H. Sadeghi, J. Shi, Z. Xiao, W. Hong, C. J. Lambert, S. Liu, *Angew. Chem.* **2016**, 56.
- [49] L. Rincon-Garcia, A. K. Ismael, C. Evangeli, I. Grace, G. Rubio-Bollinger, K. Porfyrakis, N. Agrait, and C. J. Lambert, *Nat Mater.* **2016**, 15.
- [50] D. Z. Manrique, Q. Al-Galiby, W. Hong, C.J. Lambert, *Nano Lett.* **2016**, 16, 2.
- [51] M. Famili, I.M. Grace, H.Sadeghi, C.J. Lambert, *Chem. Phys. Chem.* **2017**.
- [52] H. Sadeghi, S. Sangtarash, and C. J. Lambert, *J. Nano Lett.* **2015**, 15.
- [63] T. Meier, F. Menges, P. Nirmalraj, H. Hölscher, H. Riel, B. Gotsmann, *Phys. Rev. Lett.* **2014**, 113, 6.

### **The table of contents entry**

**The thermoelectric performance of thiophene molecular wires can be enhanced by ethylenedioxy substitution,** to yield ethylenedioxythiophene (EDOT) molecular wires, whose electrical conductance decays slowly with length and whose thermal conductance is reduced.

ToC figure





## **Supporting Information**

### **Towards high thermoelectric performance of thiophene and ethylenedioxythiophene (EDOT) molecular wires.**

Marjan Famili, Iain M. Grace, Qusiy Al-Galiby, Hatef Sadeghi and Colin J. Lambert

#### **1. Phonon transmission coefficient**

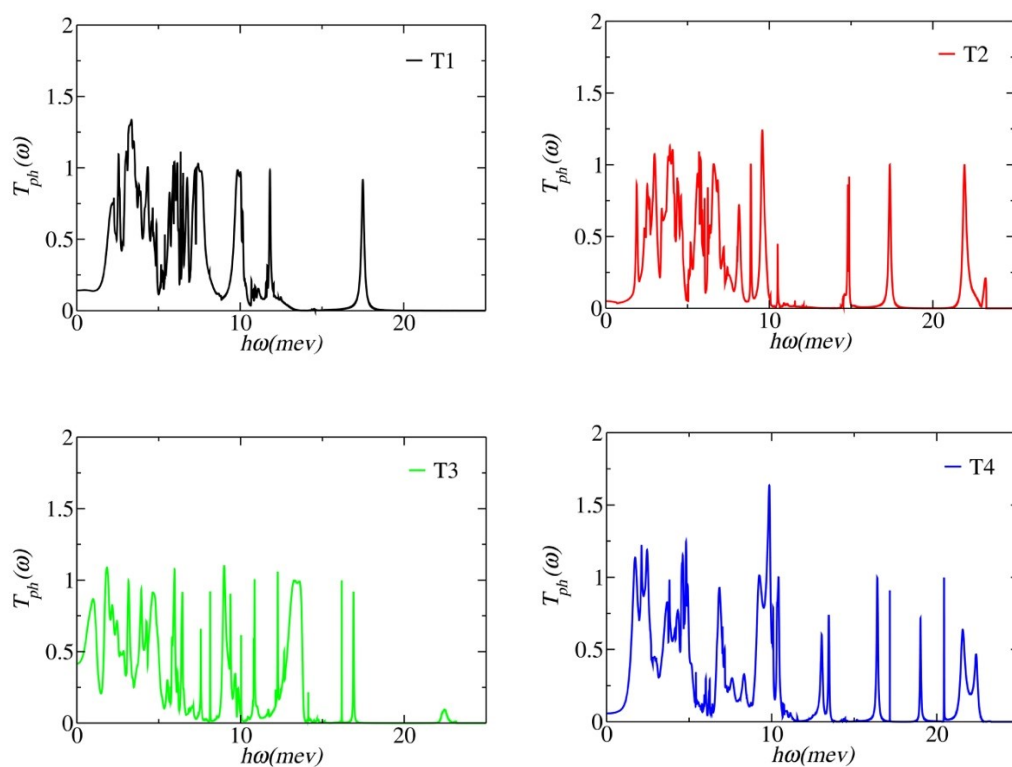


**Figure S1:** Phonon transport through the thiophene series.

Increasing the length of molecular wire affects the transmission coefficient in two ways. First the resonances become narrower as the length of the molecule increases. Second, the frequencies of vibrational modes decreases, therefore new modes (resonances in the transmission function) enter the Debye frequency window of the gold (23 meV in the present calculations). This trend can be followed in figure S1. These two factors control the area under the phonon transmission curves and therefore integral in equation (6). Figure 4 b in the manuscript, shows that the phonon conductance for the thiophene series initially drops for T2 and then increase for T3 and T4.

Similar result applies for the EDOT group. The phononic transmission coefficient of EDOT series is shown in figure S2. As the length of the EDOT increases (E1, E2, E3 and E4) the number of resonances within the Debye frequency of the gold increases. This trend, has direct effect on the phonon thermal conductance through each molecule. (figure 4b)

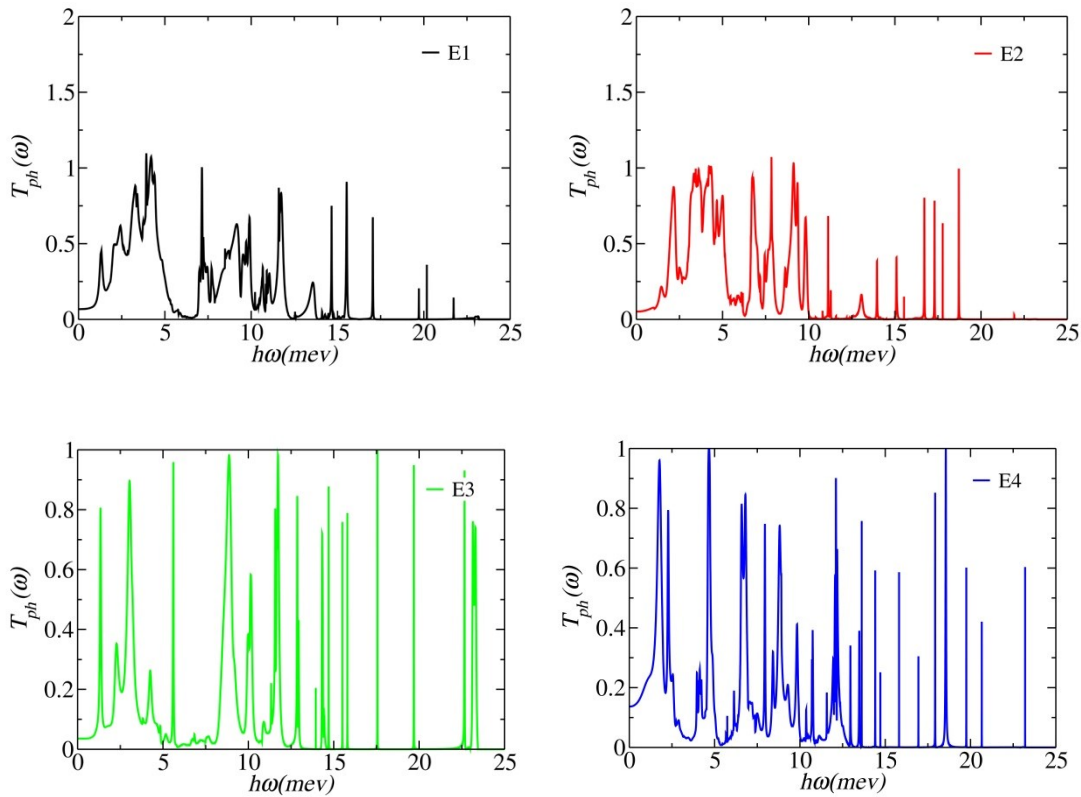


**Figure S2:** Phonon transmission through the EDOT of different length.

## 2. The Fermi energy

We have chosen the Fermi energy in our calculation such that the Seebeck coefficient of T1 is in a reasonable agreement with the measured values in the literature.

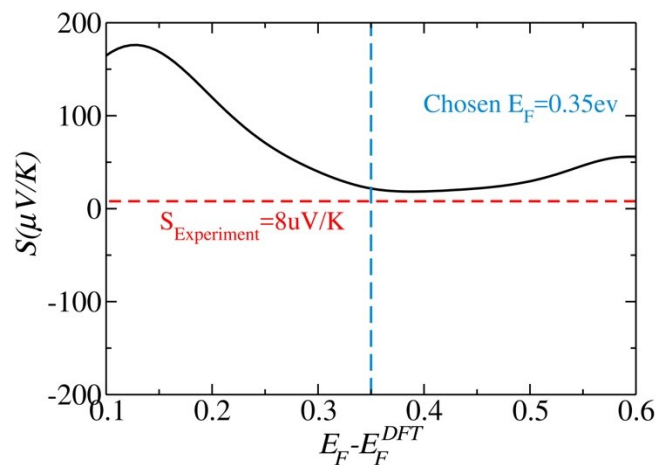


**Figure S3:** The Seebeck coefficient of T1 (black), Experimental value for the Seebeck coefficient of T1 (red) and the relatively chosen Fermi energy.

## 3. The role of anchor groups

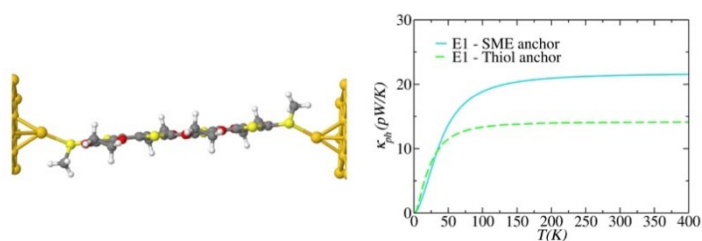


**Figure S4.** A comparison between the phonon thermal conductances of E1 with thiol and SME anchors.